Electrocardiography-Based Assessment of Cardiac Contractility

Mously D Diaw[1,2], Idriss Ngomseu Tchoupe[2], Stéphane Papelier[1], Alexandre Durand-Salmon[1], Jacques Felblinger[2,3], Julien Oster[2,3]

[1] Cardiabase, Banook Group, Nancy, France
[2] IADI, U1254, Inserm, Université de Lorraine, Nancy, France
[3] CIC-IT 1433, Université de Lorraine, Inserm, CHRU de Nancy, Nancy, France

Abstract

Heart failure is a major health concern that often follows left ventricular systolic dysfunction (LVSD) whose early identification could allow better disease management. Echocardiography is the primary diagnostic tool of LVSD, defined as reduced left ventricular ejection fraction (LVEF). Given the cost and practical limitations of echocardiography, our study investigates whether electrocardiography (ECG) could be used to estimate LVEF, making it a viable pre-screening test of LVSD.

ECG parameters including intervals and global electric heterogeneity (GEH) parameters were extracted for each of the 128 patients in PhysioNet's SHAREE database with matched ECG and LVEF. Since the orthogonal XYZ leads from which GEH parameters are typically derived were not available in SHAREE, we formed pseudo-orthogonal leads from the only 3 leads available: X ≈ V5, Y ≈ III and Z ≈ -V3. We divided the 128 subjects in half and trained different machine learning models on the first split to estimate LVEF based on the extracted ECG parameters.

The best performing ECG-based LVEF estimator, a ridge regression model, yielded a mean absolute error of 9.5%, 95% CI [8.1%, 11.3%] on the evaluation set. Our study thus suggests that the ECG could be a practical tool to gain insight on cardiac contractility, specially amongst asymptomatic individuals.

1. Introduction

Left ventricular systolic dysfunction (LVSD) refers to an impaired contraction of the left ventricle and can lead to heart failure and death [1,2]. Early identification of LVSD, which often remains asymptomatic for years, is therefore crucial to mitigate associated risks with adequate therapy. LVSD is most commonly diagnosed through echocardiography where it is defined as reduced left ventricular ejection fraction (LVEF)—different cut-offs have been used to define LVEF reduction, typically ranging from $\leq 35\%$ to $\leq 50\%$. However, echocardiography-based screening of asymptomatic individuals is not cost-effective, and the criteria for selecting potential high-risk individuals to screen remain unclear.

Unlike echocardiography, electrocardiography (ECG) is cheap, routinely available and requires little technical training, making it an attractive tool for pre-screening LVSD. Studies have suggested an association between cardiac contractility and ECG intervals like the QT [3] or ECG-derived global electric heterogeneity (GEH) parameters [4]. Convolutional neural networks (CNNs) were also suggested to identify abnormal LVEFs from ECGs ($\leq 35\%$ [5], $\leq 50\%$ [6]). Though the CNNs seem promising, their lack of interpretability could hinder clinical adoption. Indeed, it is not obvious which ECG patterns the CNNs associate with cardiac contractility.

In this work, we investigate whether LVEF could be estimated from a set of explicit ECG parameters using a machine learning approach. To this aim, we considered two types of ECG features: ECG intervals and GEH parameters derived from pseudo-orthogonal leads—truly orthogonal leads were not available in the data used in our study.

2. Method

2.1. Data

The SHAREE database [7] published on PhysioNet [8] was initially developed to investigate the usefulness of heart rate variability analysis in identifying hypertensive subjects at higher risk of developing vascular events. It includes 24-h ECG Holter recordings of 139 hypertensive subjects aged 55 and over (49 females and 90 males, 72 ± 7 years on average) recruited in 2012-2013 at the Centre of Hypertension of the University Hospital Federico II, Naples, Italy. The ECGs were recorded following a one-month anti-hypertensive therapy wash-out and are composed of 3 leads (III, V3, V5) sampled at 128 Hz. Each individual recording is associated with clinical information like echocardiographic parameters. 128 subjects had an ECG effectively matched to a LVEF value.

2.2. ECG pre-processing and delineation

We extracted 1-minute ECG segments every hour between 5 p.m. and 4 a.m. from each individual 24-h ECG recording. These segments were then upsampled to 500 Hz and smoothed following a moving average method with a window size of 15 samples. Finally, an average of the most representative heartbeats was computed for each 1-minute segment.

To delineate the average heartbeats, we used a modified version of the residual neural network (ResNet) we initially proposed to estimate the QT interval [9]. The ResNet automatically detects the following ECG fiducials: P wave onset, QRS onset and offset, T wave peak and offset.

2.3. Extraction of ECG Parameters

Using the ECG fiducials automatically detected by the aforementioned ResNet model, we derived the following parameters:

(a) ECG intervals: PR, QRS, JT_{peak}, $\text{T}_{peak}\text{T}_{end}$ and QT

(b) Global electric heterogeneity (GEH) parameters: GEH is based on the concept of the spatial ventricular gradient (SVG) and characterizes the degree of heterogeneity of total recovery time across the ventricles. We refer the reader to [10, 11] for a thorough review of SVG and GEH concepts.

Suppose X, Y and Z, three othogonal or pseudo-orthogonal leads. We denote the QRS vector $\mathbf{V}_{QRS}$ = ($\mathbf{V}_{QRS,x}$, $\mathbf{V}_{QRS,y}$, $\mathbf{V}_{QRS,z}$) and the T vector $\mathbf{V}_T$ = ($\mathbf{V}_{T,x}$, $\mathbf{V}_{T,y}$, $\mathbf{V}_{T,z}$), with $\mathbf{V}_x$, $\mathbf{V}_y$ and $\mathbf{V}_z$ their projection on the X, Y and Z axis respectively. These vectors can be computed in 2 ways:

(i) Peak vector $\mathbf{V}^{peak}$ = (X^{peak}, Y^{peak}, Z^{peak}) with X^{peak}, Y^{peak} and Z^{peak} the amplitude of the signal X, Y and Z at QRS or T peak

(ii) Mean vector $\mathbf{V}^{mean}$ = (AUC_x, AUC_y, AUC_z) with AUC_x, AUC_y and AUC_z the area under the QRS or T wave in X, Y and Z.

The spatial ventricular gradient vector corresponds to $\mathbf{V}_{SVG}$ = $\mathbf{V}_{QRS}$ + $\mathbf{V}_T$. For each vector $\mathbf{V}_{QRS}^{peak}$, $\mathbf{V}_{QRS}^{mean}$, $\mathbf{V}_T^{peak}$, $\mathbf{V}_T^{mean}$, $\mathbf{V}_{SVG}^{peak}$ and $\mathbf{V}_{SVG}^{mean}$, we compute the euclidean norm $\|\mathbf{V}\|$, the azimuth $\alpha(\mathbf{V})$ and the elevation $\varepsilon(\mathbf{V})$. We also compute:

- $W = \|\mathbf{V}_{QT}^{mean}\|$, Wilson's ventricular gradient
- $\theta_{QRS,T}^{peak}$ and $\theta_{QRS,T}^{mean}$ the QRS-T angle for peak and mean vectors respectively
- $AUC_{QRS,vmag}$, $AUC_{T,vmag}$ and $AUC_{QT,vmag}$ the AUCs computed from the vector magnitude lead.

Since Frank XYZ leads were not available in the SHAREE database, we formed pseudo-orthogonal leads from the 3 leads available: X ≈ V5, Y ≈ III and Z ≈ -V3.

2.4. ECG-based LVEF estimator

Features. We considered the following 37 features as inputs of our LVEF estimator: PR, QRS, JT_{peak}, $\text{T}_{peak}\text{T}_{end}$ and QT intervals, $\|\mathbf{V}_{SVG}^{peak}\|$, $\|\mathbf{V}_{QRS}^{peak}\|$, $\|\mathbf{V}_{QRS}^{mean}\|$, $\|\mathbf{V}_T^{peak}\|$, $\|\mathbf{V}_T^{mean}\|$, $\alpha(\mathbf{V}_{QRS}^{peak})$, $\alpha(\mathbf{V}_{QRS}^{mean})$, $\alpha(\mathbf{V}_T^{peak})$, $\alpha(\mathbf{V}_T^{mean})$, $\alpha(\mathbf{V}_{SVG}^{peak})$, $\alpha(\mathbf{V}_{SVG}^{mean})$, $\varepsilon(\mathbf{V}_{QRS}^{peak})$, $\varepsilon(\mathbf{V}_{QRS}^{mean})$, $\varepsilon(\mathbf{V}_T^{peak})$, $\varepsilon(\mathbf{V}_T^{mean})$, $\varepsilon(\mathbf{V}_{SVG}^{peak})$, $\varepsilon(\mathbf{V}_{SVG}^{mean})$, $AUC_{QRS,x}$, $AUC_{QRS,y}$, $AUC_{QRS,z}$, $AUC_{T,x}$, $AUC_{T,y}$, $AUC_{T,z}$, $AUC_{QT,x}$, $AUC_{QT,y}$, $AUC_{QT,z}$, W, $\theta_{QRS,T}^{peak}$, $\theta_{QRS,T}^{mean}$, $AUC_{QRS,vmag}$, $AUC_{T,vmag}$ and $AUC_{QT,vmag}$.

Machine learning (ML) models. Using Python's Scikit-learn library, we compared models for LVEF estimation: linear regression (**Linear**), ridge regression (**Ridge**) and support vector regression (**SVR**). For the SVR model, we tested 3 different kernels, namely linear, polynomial (of degree 2) and radial basis function (RBF).

Hyperparameter optimization. We split the 128 subjects with matched ECG and LVEF in the SHAREE database in two splits of equal size S_1 and S_2. When applicable, we optimized the hyperparameters of the ML models through grid-search on S_1, which was split into training and validation sets of equal size for this purpose. We kept the parameters yielding the lowest mean absolute error (MAE) and the highest Pearson correlation coefficient (r) on the validation set. Prior to model fitting, the ECG features were transformed with a robust scaler.

Evaluation. For bootstrap evaluation of the models, we resampled S_1 with replacement (same size) 1000 times. Each time, we fitted the given model on the resampled version of S_1 and evaluated it on S_2. All average ECG heartbeats extracted between 5 p.m. and 4 a.m. were included in the training (S_1) and test (S_2) sets. When not bootstrapping, we trained a single model on all 64 subjects in S1 without resampling. In addition to MAE and r scores, we also computed root mean squared errors (RMSE).

3. Results

Table 1 details the bootstrap scores of each ML model on S_2. The Ridge model performs best, yielding a mean absolute error of 9.5%, 95% CI [8.1%, 11.3%]. Figure 1.A shows the Bland-Altmann plot and scatterplot between the ground-truth and LVEF predictions for all average ECG heartbeats extracted between 5 p.m. and 4 a.m. and obtained with the Ridge model trained on the whole S_1 (without resampling). Overall, the model yields good LVEF estimates though lower LVEF values seem more difficult to predict from the ECG parameters. This is possibly because these abnormal cases were less represented in the SHAREE database and, subsequently, in the training set. Indeed, there were only 6/64 subjects with a LVEF $\leq 45\%$ in S_1 (11/64 in S_2).

Figure 1.B shows that the 10 most important ECG features to the Ridge model are, in this order: $AUC_{QRS,vmag}$, $\|\mathbf{V}_{QRS}^{peak}\|$, $\|\mathbf{V}_T^{mean}\|$, PR, $\varepsilon(V_{SVG}^{mean})$, $\|\mathbf{V}_T^{peak}\|$, $AUC_{T,vmag}$, $\varepsilon(V_T^{peak})$, $\alpha(V_T^{peak})$ and $\alpha(V_T^{mean})$.

Table 1. Bootstrap results.

Model	Kernel	Regularization	MAE [95% CI]	RMSE [95% CI]	r [95% CI]
Linear	–	–	17.419% [11.88%, 25.19%]	21.137% [15.38%, 28.7%]	0.096 [-0.21, 0.39]
Ridge	–	α = 34	**9.489% [8.12%, 11.27%]**	**12.542% [10.59%, 14.93%]**	**0.356 [0.09, 0.53]**
SVR	Linear	C = 0.2	9.663% [8.04%, 11.94%]	12.976% [10.68%, 15.9%]	0.314 [0.05, 0.5]
SVR	Polynomial	C = 19	12.613% [9.7%, 16.01%]	16.282% [12.76%, 20.3%]	0.259 [-0.04, 0.49]
SVR	RBF	C = 3	11.492% [8.85%, 14.55%]	15.114% [11.72%, 18.78%]	0.298 [0.01, 0.52]

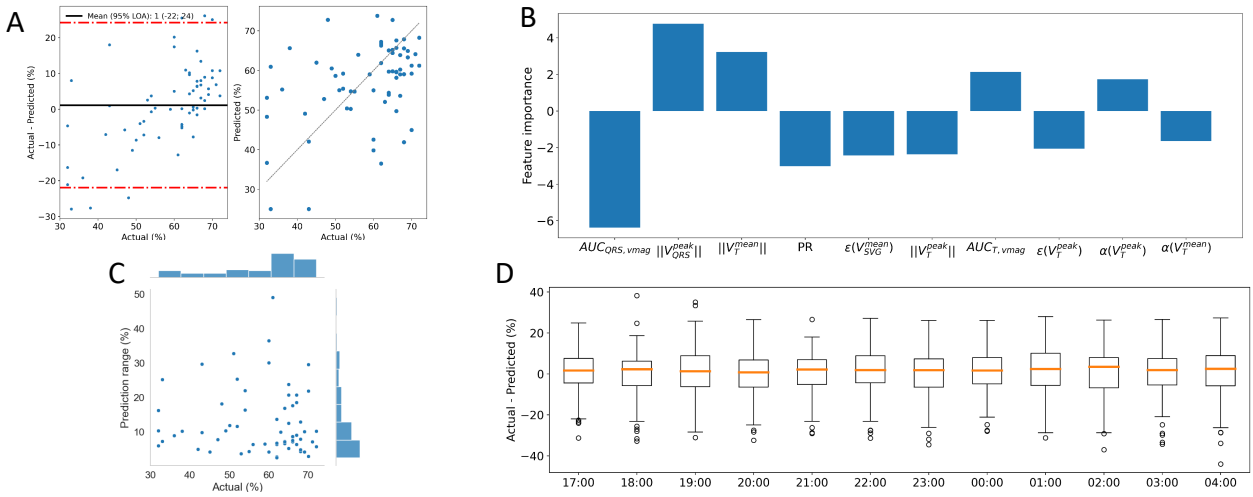

Figure 1. Evaluation of the Ridge model on S_2. **A,** Bland-Altmann plot (left) and scatterplot (right) of actual versus predicted LVEF (N = 768). The black line on the Bland-Altmann plot corresponds to the mean difference between actual and predicted LVEF and the red lines to the limits of agreement (LOA: mean ± 1.96 std). The black line on the scatterplot corresponds to an ideal fit where actual and predicted LVEF are in perfect agreement (y=x). Predictions were made for each of the N = 12x64 = 768 average ECG heartbeats extracted between 5 p.m. and 4 a.m. for each subject in S_2. **B,** Top 10 of ECG features based on ridge coefficients. **C,** Prediction range vs actual LVEF (N = 64). The former is computed as the difference between the maximum and minimum LVEF predictions for a given Holter recording. **D,** Differences between actual and predicted LVEF across ECG extraction timepoints.

Figure 1.C shows that the Ridge model is fairly consistent in predicting the LVEF from average ECG heartbeats extracted from the same individual Holter recording. Indeed, except for few cases, the prediction ranges, computed as the differences between maximum and minimum predictions, are reasonable, generally lower than 15%. This is further illustrated in Figure 1.D, which shows that the performance of the model on S_2 is consistent across ECG extraction timepoints.

4. Discussion

Our results suggest that by leveraging ECG intervals and GEH parameters, we could obtain fairly accurate LVEF estimates. To our knowledge, this is the first study to propose direct LVEF estimation based on these ECG parameters. Indeed, many studies have investigated whether the ECG could serve for early diagnosis of cardiac contractile dysfunction but most have focused on LVEF classification [5,6,12–15]. Alkhodari et al. [15] also leveraged heart rate variability features to build a LVEF regressor.

Because the mechanical activity of the heart stems from electrical excitation, it is reasonable to assume that cardiac structural changes are reflected on the ECG. The 2 most important ECG features to the Ridge model are related to the QRS amplitude and area (cf. Figure 1.B). This might further confirm the association between subtle QRS changes and LVEF reduction [16]. Futhermore, 6 out of the 10 most important features are specific to the T wave. This is consistent with other studies that found a relationship between repolarization heterogeneity and mechanical dispersion [3, 11, 17].

Though our model does not seem to be drastically impacted by the time of ECG sampling, the few cases where the prediction range for a given 24-h Holter is significant (cf. outliers in Figure 1.C) could be explained by circadian changes of the LVEF [18] or the use of non-resting ECG segments. In the latter case, we could improve our ECG pre-processing pipeline to only estimate LVEF based on resting ECG data.

5. Conclusion

In this study, we showed that ECG intervals and GEH parameters—some of which have been shown to be associated with myocardial mechanics—are useful to esti-

mate LVEF. Overall, our model is fairly accurate, specially when predicting normal to mid-range LVEF values. This ECG-based LVEF estimator could therefore be a viable tool to monitor subtle changes in cardiac contractility. In the future, we will explore the estimation of other echocardiographic parameters, like global longitudinal strain, that are more representative of contractility than LVEF.

This study will be followed by a local clinical study (CHRU de Nancy) to assess the usefuleness of our method in detecting cardiac contractile dysfunction in a high-risk population with no diagnosed ECG abnormalities.

Acknowledgments

This work was supported in part by Banook Group and in part by the French National Association for Research and Technology (ANRT, CIFRE) under Grant 2021/1466.

References

[1] Wang TJ, Evans JC, Benjamin EJ, Levy D, LeRoy EC, Vasan RS. Natural history of asymptomatic left ventricular systolic dysfunction in the community. Circulation 2003; 108(8):977–982.

[2] Echouffo-Tcheugui JB, Erqou S, Butler J, Yancy CW, Fonarow GC. Assessing the risk of progression from asymptomatic left ventricular dysfunction to overt heart failure: a systematic overview and meta-analysis. JACC Heart Failure 2016;4(4):237–248.

[3] Verdugo-Marchese M, Coiro S, Selton-Suty C, Kobayashi M, Bozec E, Lamiral Z, Venner C, Zannad F, Rossignol P, Girerd N, et al. Left ventricular myocardial deformation pattern, mechanical dispersion, and their relation with electrocardiogram markers in the large population-based STANISLAS cohort: insights into electromechanical coupling. European Heart Journal Cardiovascular Imaging 2020;21(11):1237–1245.

[4] Biering-Sørensen T, Kabir M, Waks JW, Thomas J, Post WS, Soliman EZ, Buxton AE, Shah AM, Solomon SD, Tereshchenko LG. Global ECG measures and cardiac structure and function: the ARIC study (Atherosclerosis Risk in Communities). Circulation Arrhythmia and Electrophysiology 2018;11(3):e005961.

[5] Attia ZI, Kapa S, Lopez-Jimenez F, McKie PM, Ladewig DJ, Satam G, Friedman PA. Screening for cardiac contractile dysfunction using an artificial intelligence–enabled electrocardiogram. Nature medicine 2019;25(1):70–74.

[6] Sun JY, Qiu Y, Guo HC, Hua Y, Shao B, Qiao YC, Wang RX. A method to screen left ventricular dysfunction through ECG based on convolutional neural network. Journal of Cardiovascular Electrophysiology 2021;32(4):1095–1102.

[7] Melillo P, Izzo R, Orrico A, Scala P, Attanasio M, Mirra M, De Luca N, Pecchia L. Automatic prediction of cardiovascular and cerebrovascular events using heart rate variability analysis. PloS one 2015;10(3):e0118504.

[8] Goldberger A, Amaral L, Glass L, Hausdorff J, Ivanov PC, Mark R, Stanley HE. PhysioBank, PhysioToolkit, and PhysioNet: Components of a New Research Resource for Complex Physiologic Signals. Circulation 2000;101(23):e215–e220.

[9] Diaw MD, Papelier S, Durand-Salmon A, Felblinger J, Oster J. AI-Assisted QT Measurements for Highly Automated Drug Safety Studies. IEEE Transactions on Biomedical Engineering 2023;70(5):1504–1515.

[10] Waks JW, Tereshchenko LG. Global electrical heterogeneity: A review of the spatial ventricular gradient. Journal of electrocardiology 2016;49(6):824–830.

[11] Tereshchenko LG. Global electrical heterogeneity: mechanisms and clinical significance. Computing in Cardiology 2018;45:1–4.

[12] Cho J, Lee B, Kwon JM, Lee Y, Park H, Oh BH, Jeon KH, Park J, Kim KH. Artificial intelligence algorithm for screening heart failure with reduced ejection fraction using electrocardiography. ASAIO Journal 2021;67(3):314–321.

[13] Potter EL, Rodrigues CHM, Ascher DB, Abhayaratna WP, Sengupta PP, Marwick TH. Machine learning of ECG waveforms to improve selection for testing for asymptomatic left ventricular dysfunction. Cardiovascular Imaging 2021;14(10):1904–1915.

[14] Golany T, Radinsky K, Kofman N, Litovchik I, Young R, Monayer A, Love I, Tziporin F, Minha I, Yehuda Y, et al. Physicians and Machine-Learning Algorithm Performance in Predicting Left-Ventricular Systolic Dysfunction from a Standard 12-Lead-Electrocardiogram. Journal of Clinical Medicine 2022;11(22):6767.

[15] Alkhodari M, Jelinek HF, Werghi N, Hadjileontiadis LJ, Khandoker AH. Estimating left ventricle ejection fraction levels using circadian heart rate variability features and support vector regression models. IEEE Journal of Biomedical and Health Informatics 2020;25(3):746–754.

[16] García-Escobar A, Vera-Vera S, Jurado-Román A, Jiménez-Valero S, Galeote G, Moreno R. Subtle QRS changes are associated with reduced ejection fraction, diastolic dysfunction, and heart failure development and therapy responsiveness: Applications for artificial intelligence to ECG. Annals of Noninvasive Electrocardiology 2022;27(6):e12998.

[17] Sauer AJ, Selvaraj S, Aguilar FG, Martinez EE, Wilcox JE, Passman R, Goldberger JJ, Freed BH, Shah SJ. Relationship between repolarization heterogeneity and abnormal myocardial mechanics. International journal of cardiology 2014;172(1):289–291.

[18] Veale D, Fagret D, Pepin JL, Bonnet C, Siche JP, Lévy P. Circadian changes of left ventricular ejection fraction in normal subjects. Chronobiology International 1994; 11(3):200–210.

Address for correspondence:

Julien Oster (julien.oster@inserm.fr)
Laboratoire IADI (Inserm U1254)
Bâtiment Recherche, CHRU Nancy-Brabois, Rue du Morvan
54500 Vandoeuvre, France